PHYSICAL REVIEW E **68**, 060401(R) (2003)

Structure and melting of two-species charged clusters in a parabolic trap

J. A. Drocco,[1] C. J. Olson Reichhardt,[2] C. Reichhardt,[2] and B. Jankó[1]
[1]*Department of Physics, University of Notre Dame, Notre Dame, Indiana 46556, USA*
[2]*Theoretical Division, Los Alamos National Laboratory, Los Alamos, New Mexico 87545, USA*
(Received 12 September 2003; published 24 December 2003)

We consider a system of charged particles interacting with an unscreened Coulomb repulsion in a two-dimensional parabolic confining trap. The static charge on a portion of the particles is twice as large as the charge on the remaining particles. The particles separate into a shell structure with those of greater charge situated farther from the center of the trap. As we vary the ratio of the number of particles of the two species, we find that for certain configurations, the symmetry of the arrangement of the inner cluster of singly charged particles matches the symmetry of the outer ring of doubly charged particles. These matching configurations have a higher melting temperature and a higher thermal threshold for intershell rotation between the species than the nonmatching configurations.

DOI: 10.1103/PhysRevE.68.0604XX PACS number(s): 82.70.Dd, 64.60.Cn, 83.10.Mj

Clusters of repulsive particles in confined traps have attracted considerable attention recently due to their applicability to a wide variety of systems. For example, two-dimensional (2D) clusters can represent electrons in quantum dots [1] or on the surface of liquid helium [2], vortices in superfluids [3], colloidal particles in circular traps [4], confined ferromagnetic particles [5], and charged dust particles in plasma traps [6]. The 2D charged clusters also resemble the problem of charge distribution studied by Thomson in his ''plum-pudding'' model of the atom [7].

When confined to a parabolic trap, charged particles form a structure of concentric rings, with the inner particles forming a distorted triangular lattice resembling a defected Wigner crystal and the outer rings taking on a more circular shape that conforms to the radial symmetry of the trap [8,9]. Among the possible charge configurations are several ''magic'' arrangements in which the number of particles is such that the shells form with only a few symmetrically distributed dislocations, and so have a reduced total energy compared to what is predicted based on a semiempirical approximation [10]. Bubeck *et al.* [4] have observed that certain colloidal clusters confined by a circular hard-wall trap exhibit *two-stage* melting. As the temperature is increased in their experiment, intershell rotation between the outer two shells first occurs, destroying the angular order of the system. Angular order is then restored, until at higher temperatures complete melting occurs.

Several explanations of this two-stage melting phenomenon have been proposed [8,9,11,12], all of which focus on the intershell rotation which occurs prior to the exchange of particles between shells. Most plausible among these is the theory that the rotation is due to an incommensuration between the shapes of the potentials created by the adjacent shells. For this intershell rotation to occur, the inner-shell configuration must be sufficiently stable to have a melting temperature higher than the threshold for intershell rotation.

In our simulation, we extend the confined charge system to include particles with two distinct values of charge. We find that the two species separate into shells, with those of greater charge located farther from the center of the trap. Since the particles have a long-range repulsive interaction, the lowest-energy configuration places the stronger charges as far apart as possible. If two-stage melting and intershell rotation are caused by an incommensuration between the potentials formed by the particles, then we should be able to predict the occurrence of intershell rotation based on the ratio of particles in the outer shell of singly charged particles to the number of doubly charged particles.

We consider a system of N_s+N_d charged particles interacting via an unscreened $1/r$ Coulomb repulsion, where N_s is the number of single-charge particles with $q_s=1$ and N_d is the number of doubly charged particles with $q_d=2$. The particles are free to move in two dimensions but are confined by a parabolic trap centered at the origin and increasing radially as r^2. The dimensionless Hamiltonian [9] for this system is

$$H=\sum_{i=1}^{N_s+N_d}\sum_{j=i+1}^{N_s+N_d}\frac{q_i q_j}{|\vec{r}_i-\vec{r}_j|}+A\left(\sum_{i=1}^{N_s+N_d}|\vec{r}_i|^2\right), \qquad (1)$$

where q_i ($\vec{r}_i$) is the charge (position) of particle i and we fix the strength of the parabolic trap to $A=10$. Charged colloidal particles in a confinement potential, such as those of Wei *et al.* [13], bear the closest resemblance to the Coulomb interaction used in this study.

Using a molecular dynamics simulation method, we initialize the system at high temperature, simulated by random Langevin kicks, and then slowly anneal it to a $T=0$ ground-state configuration. We checked the accuracy of this method by reproducing the ground-state configurations for single-species particle clusters found by Kong *et al.* [14], albeit with different confinement strengths. Once we have obtained the ground states of the two-species clusters, we slowly increase the temperature and observe the melting of the system.

Figure 1 shows several examples of the ground-state configurations we obtained for $N_d=5$, 6, and 7, respectively. The structure of the inner core of singly charged particles is altered both by the presence and by the number of doubly charged particles that are present. For $N_d=5$, configurations with $N_s=6$, 11, and 31 have fivefold symmetry matching the number of doubly charged particles in the outer shell. N_s

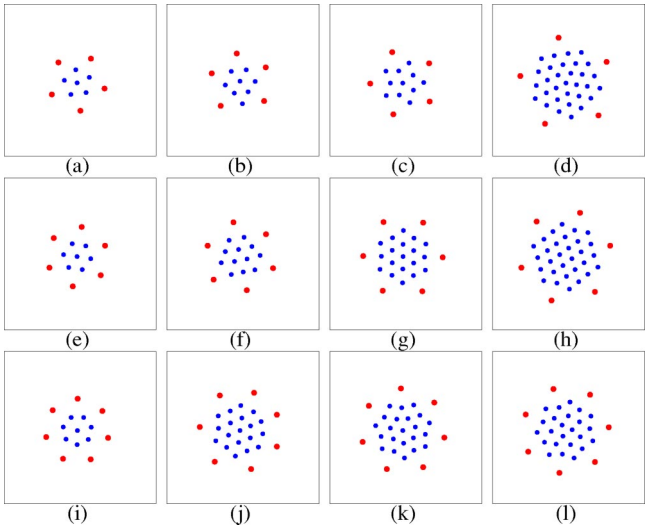

FIG. 1. Ground-state colloid configurations for (a)–(d) $N_d=5$, (e)–(h) $N_d=6$, and (i)–(l) $N_d=7$, with $N_s=$(a) 6, (b) 8, (c) 11, (d) 31, (e) 7, (f) 12, (g) 19, (h) 30, (i) 8, (j) 19, (k) 22, (l) 24. Small dots are the singly charged particles and large dots are the doubly charged particles.

$=8$ approximates a sixfold symmetric arrangement by substituting a singly charged particle to fill a potential well in the outermost shell. For $N_d=6$, configurations with $N_s=7$ and $N_s=19$ have sixfold symmetry. Configurations with $N_s=12$ and $N_s=27$ have threefold symmetry and the configuration with $N_s=30$ has twofold symmetry, which also are commensurate with the arrangement of particles in the outer shell. For $N_d=7$, $N_s=8$ and 22 are the only sevenfold symmetric inner particle configurations. $N_s=23$ and 24 are nearly symmetric, with sevenfold symmetry in the outer two shells of the inner particle configuration.

In general we find highly ordered structures when the smaller particles form a commensurate structure with the outer particles. All the configurations are shown in Ref. [15]. The general expressions $N_s=kN_d$ and $N_s=kN_d+1$, with k a small integer, predict some configurations that have rotational symmetry through an angle $2\pi/N_d$, such as $N_d=5$, $N_s=6$, but do not hold for all values of k due to the fact that the outer particles may distort from a uniformly spaced arrangement in order to better accommodate the inner particles. For example, at $N_d=5$, $N_s=8$ [Fig. 1(b)], a small charge moves to the outer ring. This can be simply understood in terms of angular stiffness of the rings. The radius of the outer ring increases as N_s increases, but since N_d is fixed, the large charges move further apart, decreasing the angular stiffness of the outer ring and making it susceptible to angular compressions that permit the intrusion of a small charge. A similar but opposite process occurs for the inner ring of small charges. As N_s increases, the number of small charges around the ring increases until the angular stiffness of the ring is so large that it is not possible to compress it enough to add another small charge, and the next charge must move out into a new ring.

Although in this work we only present results for $q_d=2q_s$, we have considered other charge ratios, and find that

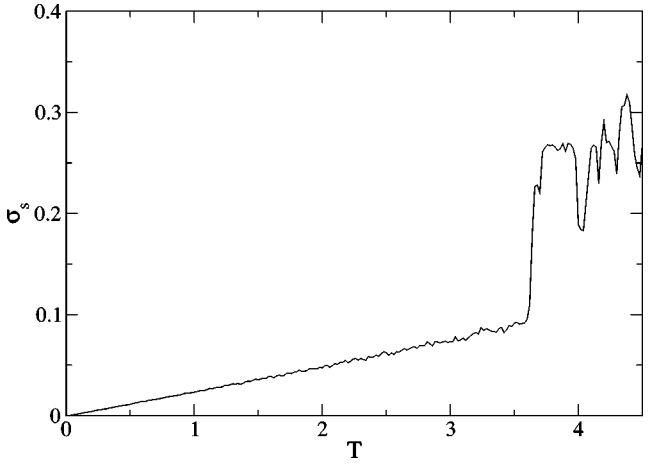

FIG. 2. Plot of σ_s vs temperature for $N_d=6$, $N_s=7$, averaged over five realizations.

the more highly charged particles always move to the outside of the trap and the same general commensurate-incommensurate phases occur. We have also performed simulations with larger $N_d>7$; however, we do not treat this case here since the outer particles begin to form multiple rings which have their own commensurate-incommensurate transitions. In addition, we have run a set of simulations for $N_s<15$ with the same trap but with a $1/r^3$ interparticle interaction potential, which corresponds to the interaction between magnetic colloids. We found that, in general, the ground states and also the dynamical properties were qualitatively identical to those in the case of Coulomb repulsion for small N_s ($N_s<15$).

In order to confirm whether the highly ordered commensurate phases are more stable we consider the melting of the two-species system. We determine the temperature T_e of the first exchange of particles between shells by measuring intershell exchange of the singly charged particles,

$$\sigma_s=\frac{1}{N_s}\sum_{i=1}^{N_s}|\vec{r}_i(t)-\vec{r}_i(0)|. \tag{2}$$

This gives the mean radial distance of the inner singly charged particles from their initial $T=0$ positions. The slow increase in σ_s at low temperatures corresponds to the small radial distortions of the configuration introduced by the random Langevin kicks, which increase in size as the temperature increases. The overall configuration remains fairly stiff at these low temperatures. σ_s shows a marked increase at T_e when the inner particles begin to jump between shells, as illustrated in Fig. 2 for a system with $N_s=7$ and $N_d=6$. This configuration is highly stable, as shown in Fig. 1(e), with one central particle surrounded by an inner hexagonal shell of six singly charged particles and an outer hexagonal shell of six doubly charged particles. At $T=3.55$, σ_s jumps when one of the first-shell particles exchanges with the central particle, as shown in the trajectories of Fig. 3.

A similar measure, σ_d, tracks the doubly charged particles; however, as they never formed more than one shell for the parameters considered here, there were no intershell ex-

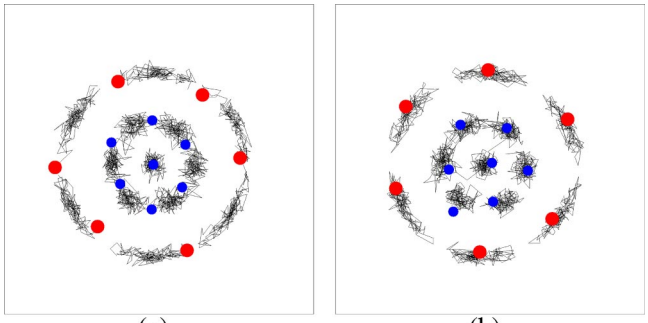

FIG. 3. Particle trajectories (lines) for $N_d=6$, $N_s=7$ at temperatures (a) $T=3.5$ with no intershell exchange and (b) $T=3.6$ with intershell exchange.

changes and σ_d only increased linearly with temperature. We observe exchanges of a singly charged particle with a doubly charged particle only at very high temperatures $T \gg T_e$, and these exchanges occur only for highly asymmetric and disordered configurations.

To track the onset temperature T_r of intershell rotation between the two species when it occurs, we use a second measure, Δ_θ:

$$\Delta_\theta = \left| \frac{1}{N_s} \sum_{i=1}^{N_s} [\theta_i(t) - \theta_i(0)] - \frac{1}{N_d} \sum_{j=1}^{N_d} [\theta_j(t) - \theta_j(0)] \right|, \tag{3}$$

which gives the difference between the mean angular displacements of the two species from their initial configurations. Δ_θ increases when the shells slip past each other, but is insensitive to coherent rotation of the two species. Δ_θ becomes meaningless if the particles do not maintain the same orientation with respect to the other particles of the same species, so it can detect intershell rotation only when this occurs *before* the onset of intershell exchange. Δ_θ also detects relative slip between shells of the same particle species, which does not interest us here. Such same-species shell slips were generally limited to the erratic rotation of two particles at the center of the configuration, and produced a sufficiently small change in Δ_θ to be distinguished easily from a genuine rotation relative to the other species. For configurations with a single central particle located roughly at the origin, the angular displacement of that particle was excluded from Δ_θ in order to reduce noise.

An example of intershell rotation measured by Δ_θ is shown in Fig. 4, where we plot Δ_θ vs temperature for a configuration of $N_s=7$ and $N_d=7$. In this case, the configurations of each of the two species are highly stable independently, with the singly charged particles forming a hexagonal ring around a central particle. However, there is an incoherence between the hexagonal ring of singly charged particles and the seven-particle ring of doubly charged particles which surrounds it. Since the onset of intershell rotation at T_r is more gradual than the intershell exchange transition, we define T_r to occur when Δ_θ exceeds a threshold value of $\Delta_\theta = \pi/N_d$, corresponding to an angular displacement of half of the angular distance between neighboring particles in the

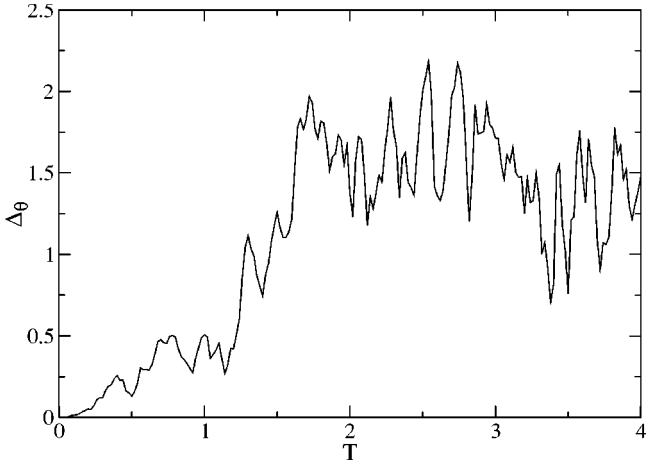

FIG. 4. Plot of Δ_θ vs temperature for $N_d=7$, $N_s=7$, averaged over five realizations.

outer shell of doubly charged particles. In Fig. 4, $\Delta_\theta = \pi/N_d$ falls at $T \approx 0.65$, corresponding to a slipping between the outer shell and the inner cluster of particles. The trajectory plot, Fig. 5, also indicates this slipping, as the trails of the inner-shell particles become larger than those of the outer-shell particles at this temperature.

The matching of the inner particle symmetry with the outer-shell symmetry produces an elevated melting threshold for commensurate configurations. The melting temperature T_m is taken to be the lower of T_e or T_r. In Fig. 6(b) we plot T_m for a range of N_s at fixed $N_d=6$. Figures 6(a) and 6(c) show T_m for $N_d=5$ and $N_d=7$, respectively. For each configuration, we averaged σ_s and Δ_θ over five realizations to reduce error. In Fig. 6(b), T_m for $N_d=6$ has a peak at $N_s=19$, another perfect triangular arrangement. We also find an elevated melting temperature for $N_d=12$, which has threefold symmetry. As seen in Fig. 6(a), configuration $N_d=5$ and $N_s=11$ also exhibits a higher than average melting temperature. This is expected since the configuration $N_s=11$ has fivefold symmetry, commensurate with the number of outer particles. Figure 6(c) shows high T_m values for $N_d=7$ at $N_s=23$ and $N_s=24$, which is expected due to the matching sevenfold symmetry of the outer three rings. The inner part of the configuration $N_d=7$, $N_s=19$ forms the same highly

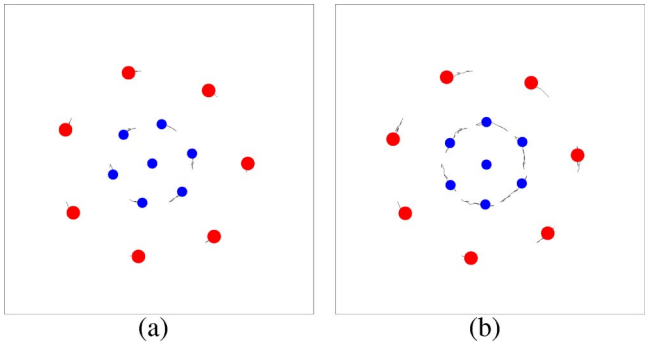

FIG. 5. Particle trajectories over a short time interval for $N_d=7$, $N_s=7$ at (a) $T=0.6$ with no intershell rotation and (b) $T=0.7$ with intershell rotation.

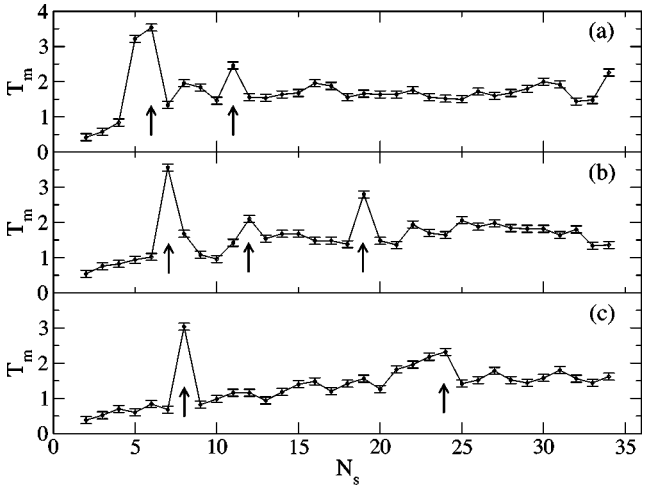

FIG. 6. Melting temperature T_m vs N_s for (a) $N_d=5$, (b) $N_d=6$, and (c) $N_d=7$.

stable perfectly hexagonal arrangement of $N_d=6$, $N_s=19$, and thus has a high threshold for intershell exchange between the singly charged inner particles. However, the incommensuration with the seven particles on the outside yields a low threshold for intershell rotation.

There is an obvious shift in the peaks of Figs. 6(a)–6(c) as the number of outer-shell doubly charged particles changes. Most notably, the highest melting temperature for each N_d occurs for $N_s=N_d+1$, when the singly charged particles form a central particle surrounded by a shell that is commensurate with the outer particles. As expected, the highest melting temperature occurs for $N_d=6$ and $N_s=7$, as this arrangement matches the triangular lattice of the Wigner crystal. However, melting temperatures nearly as high occur for $N_d=5$ and $N_s=5$ and 6. We believe that the smaller size of the crystal in this case exaggerates the effect of the commensuration between rings, despite the dissimilarity with the bulk lattice configuration.

In conclusion we have investigated the structure and melting of two species of charged particles in a parabolic trap. The more highly charged particles form an outer ring. Highly ordered clusters occur when the structure of the central cluster of singly charged particles is commensurate with the outer ring of doubly charged particles. We observe variations in the melting temperatures of the two-species clusters, with elevated melting thresholds for intershell rotation and intershell particle exchange when a commensuration occurs between the symmetry of the inner cluster and the outer ring. It may be possible to observe similar variations in melting for other confining potentials, including hard-wall potentials, and this would be an interesting direction for further research.

This work was supported by the U.S. Department of Energy under Contract No. W-7405-ENG-36 and by the U.S. DOE, Office of Science, under Contract No. W-31-109-ENG-38. B.J. and J.D. were supported by NSF-NIRT Grant No. DMR02-10519 and by the Alfred P. Sloan Foundation.

[1] M.A. Reed and W.P. Kirk, *Nanostructure Physics and Fabrication* (Academic Press, Boston, 1989).
[2] P. Leiderer, W. Ebner, and V.B. Shilkin, Surf. Sci. **113**, 105 (1987).
[3] Y. Kondo, J.S. Korhonen, M. Krusius, V.V. Dmitriev, E.V. Thuneberg, and G.E. Volovik, Phys. Rev. Lett. **68**, 3331 (1992).
[4] R. Bubeck, C. Bechinger, S. Neser, and P. Leiderer, Phys. Rev. Lett. **82**, 3364 (1999).
[5] M. Golosovsky, Y. Saado, and D. Davidov, Phys. Rev. E **65**, 061405 (2002).
[6] W-T. Juan, Z-H. Huang, J-W. Hsu, Y-J. Lai, and Lin I, Phys. Rev. E **58**, R6947 (1998).
[7] J.J. Thomson, Philos. Mag. **7**, 237 (1904); B. Partoens and F.M. Peeters, J. Phys.: Condens. Matter **9**, 5383 (1997).
[8] V.M. Bedanov and F.M. Peeters, Phys. Rev. B **49**, 2667 (1994).
[9] V.A. Schweigert and F.M. Peeters, Phys. Rev. B **51**, 7700 (1995).
[10] A.A. Koulakov and B.I. Shklovskii, Phys. Rev. B **57**, 2352 (1998).
[11] I.V. Schweigert, V.A. Schweigert, and F.M. Peeters, Phys. Rev. Lett. **84**, 4381 (2000).
[12] Y-J. Lai and Lin I, Phys. Rev. E **64**, 015601 (2001).
[13] Q.-H. Wei, C. Bechinger, D. Rudhardt, and P. Leiderer, Phys. Rev. Lett. **81**, 2606 (1998).
[14] M. Kong, B. Partoens, and F.M. Peeters, Phys. Rev. E **65**, 046602 (2002).
[15] All configurations can be seen at http://www.t12.lanl.gov/home/olson/Colloid2S.html